


Towards ultra-intense ultra-short ion beams driven by a multi-PW laser

J. Badziak and J. Domański 

Institute of Plasma Physics and Laser Microfusion, Warsaw, Poland

Research Article

Cite this article: Badziak J, Domański J (2019). Towards ultra-intense ultra-short ion beams driven by a multi-PW laser. *Laser and Particle Beams* **37**, 288–300. <https://doi.org/10.1017/S0263034619000533>

Received: 11 June 2019

Accepted: 21 June 2019

First published online: 26 July 2019

Key words:

Extreme Light Infrastructure; high-energy ion beam; laser-driven ion acceleration; laser plasma; multi-PW laser

Author for correspondence:

J. Domański, Institute of Plasma Physics and Laser Microfusion, Warsaw, Poland.

E-mail: jaroslaw.domanski@ifpilm.pl

Abstract

The multi-petawatt (PW) lasers currently being built in Europe as part of the Extreme Light Infrastructure (ELI) project will be capable of generating femtosecond light pulses of ultra-relativistic intensities ($\sim 10^{23}$ – 10^{24} W/cm²) that have been unattainable so far. Such laser pulses can be used for the production of high-energy ion beams with unique features that could be applied in various fields of scientific and technological research. In this paper, the prospect of producing ultra-intense (intensity $\geq 10^{20}$ W/cm²) ultra-short (pico- or femtosecond) high-energy ion beams using multi-PW lasers is outlined. The results of numerical studies on the acceleration of light (carbon) ions, medium-heavy (copper) ions and super-heavy (lead) ions driven by a femtosecond laser pulse of ultra-relativistic intensity, performed with the use of a multi-dimensional (2D3 V) particle-in-cell code, are presented, and the ion acceleration mechanisms and properties of the generated ion beams are discussed. It is shown that both in the case of light ions and in the case of medium-heavy and super-heavy ions, ultra-intense femtosecond multi-GeV ion beams with a beam intensity much higher (by a factor $\sim 10^2$) and ion pulse durations much shorter (by a factor $\sim 10^4$ – 10^5) than achievable presently in conventional radio frequency-driven accelerators can be produced at laser intensities of 10^{23} W/cm² predicted for the ELI lasers. Such ion beams can open the door to new areas of research in high-energy density physics, nuclear physics and inertial confinement fusion.

Introduction

High-energy ion accelerators driven by a radio-frequency (RF) electromagnetic field are basic tools for research in nuclear and particle physics, but they also have uses in high energy-density (HED) physics, materials science and medicine. They are capable of producing mono-energetic ion beams with ion energies from MeV up to multi-TeV. However, because the acceleration field strength in these accelerators cannot exceed 1 MV/cm, achieving high ion energy requires a very long acceleration path, which means that the accelerator is usually a large and fairly complex device. With their potential to be more compact and less complex, laser-driven ion accelerators are considered to be a promising alternative or supplement to RF-driven accelerators.

The laser-driven accelerator is composed of a high-intensity short-pulse laser and a target placed in a vacuum chamber. The interaction of the laser pulse with the target results in the production of hot dense plasma. Due to the action of the laser field, a part of the plasma electrons is separated from the plasma ions which results in the creation of a strong electric field between the electron layer and the ions. This field accelerates the ions, and because the field strength is extremely high (up to hundreds of GV/cm) the ions can reach high energies during very short time periods (<1 ps) and over very short (sub-mm) distances, by orders of magnitude shorter than required in RF-driven accelerators. The detailed mechanism of ion acceleration depends on both the laser pulse and the target parameters, with the acceleration mechanisms being different for different laser–target interaction conditions (Borghesi *et al.*, 2006; Badziak, 2007; Daido *et al.*, 2012; Macchi *et al.*, 2013). Currently, several ion acceleration mechanisms are known and have been extensively studied. They include: Target normal sheath acceleration (Snavely *et al.*, 2000; Wilks *et al.*, 2001; MacKinnon *et al.*, 2002; Allen *et al.*, 2004; Cowan *et al.*, 2004; Borghesi *et al.*, 2006; Fuchs *et al.*, 2006; Badziak, 2007; Daido *et al.*, 2012; Macchi *et al.*, 2013), skin-layer ponderomotive acceleration (Badziak *et al.*, 2004; 2008; Głowacz *et al.*, 2006; Badziak, 2007), radiation pressure acceleration (RPA) (Esirkepov *et al.*, 2004; Macchi *et al.*, 2005; 2013; Klimo *et al.*, 2008; Robinson *et al.*, 2008; Grech *et al.*, 2011; Daido *et al.*, 2012), laser break-out afterburner (Yin *et al.*, 2006; 2007; Daido *et al.*, 2012; Macchi *et al.*, 2013), collisionless electrostatic shock acceleration (Silva *et al.*, 2004; Daido *et al.*, 2012; Macchi *et al.*, 2013), ion solitary wave acceleration (Jung *et al.*, 2011; Yin *et al.*, 2011), Coulomb explosion acceleration (Esirkepov *et al.*, 2000; Bychenkov and Kovaliev, 2005), and laser-induced cavity pressure acceleration (Badziak *et al.*, 2012; 2013). In a real experiment, two or more of these acceleration mechanisms can contribute to the ion acceleration process (Higginson *et al.*, 2018; Qiao *et al.*, 2019).

Laser-accelerated ion beams have the potential to be applied in a variety of fields including nuclear and particle physics (Ledingham and Galster, 2010; Negoita *et al.*, 2016), HED physics

(Koenig *et al.*, 2005; Macchi *et al.*, 2013), inertial confinement fusion (ICF) (Roth *et al.*, 2001; Fernandez *et al.*, 2014), materials science (Torrisci *et al.*, 2003; Wołowski *et al.*, 2007) or nuclear medicine (Bulanov *et al.*, 2002; Fritzer *et al.*, 2003; Ledingham and Galster, 2010). To produce ion beams with parameters required for the vast majority of these applications, multi-petawatt (PW) laser drivers and ultra-relativistic laser beam intensities ($\geq 10^{23}$ W/cm²) are required. Such multi-PW lasers are currently being built at several research centers in the world, and in particular in Europe as part of the Extreme Light Infrastructure (ELI) project (Negoita *et al.*, 2016; <http://www.eli-laser.eu>). However, studies on ion acceleration in the ultra-relativistic intensity regime are still in the early stages (Esirkepov *et al.*, 2004; Yin *et al.*, 2007; Tamburini *et al.*, 2010; Zheng *et al.*, 2012; Capdessus and McKenna, 2015; Bulanov *et al.*, 2016; Domański *et al.*, 2017; Xu *et al.*, 2017) and were focused on the acceleration of protons or light ions. To understand the acceleration mechanisms and ion beam properties well enough to control the ion beam parameters at a level required for applications, much more research is necessary. This is especially true for the acceleration of heavy ions. Although the possibility of generating fast heavy ions using lasers has been demonstrated in many experiments (Clark *et al.*, 2000; Krushelnik *et al.*, 2000; Badziak *et al.*, 2001; 2007; McKenna *et al.*, 2004; Torrisci *et al.*, 2006; Braenzel *et al.*, 2015; Nishiuchi *et al.*, 2015), the parameters of the generated ion beams, especially the ion energies, were usually far from what was required for real applications because the intensities of laser pulses used in these experiments were too low. The acceleration of heavy ions to GeV or multi-GeV energies (desirable in the majority of applications) requires ultra-relativistic laser intensities that are unreachable so far, so only theoretical or numerical studies of laser-driven acceleration of heavy ions at such intensities have been possible until now. Unfortunately, the number of papers dealing with this topic is very limited (Wu *et al.*, 2014; Petrov *et al.*, 2016; 2017; Domański and Badziak, 2018; Domański *et al.*, 2018; Li *et al.*, 2019), so acceleration of heavy ions in the ultra-relativistic intensity regime is actually a very poorly explored research area in the field of laser-driven particle acceleration.

In this paper, the acceleration of light (C), medium-heavy (Cu), and heavy (Pb) ions by a multi-PW laser pulse of ultra-relativistic intensity to be available at the ELI infrastructure is investigated using an advanced multi-dimensional (2D3V) particle-in-cell (PIC) code. The ion acceleration mechanisms are analyzed and results showing various properties of the accelerated ion beams are presented and discussed. The possibility of producing ultra-intense, ultra-short (sub-picosecond) ion beams with parameters unattainable with conventional RF-driven accelerators is demonstrated and potential applications of such ion beams is briefly outlined.

Results and discussion

The numerical code and the laser and target parameters

In this paper, we investigate the acceleration of C, Cu or Pb ions by a multi-PW laser pulse with parameters corresponding to those of the ELI-NP lasers. The numerical simulations were performed using a fully electromagnetic, relativistic multi-dimensional (2D3V) PIC code (Domański *et al.*, 2017) extended with “on-line” calculations of the ionization levels of the target atoms and accelerated ions that are especially important for properly modeling the acceleration of medium-heavy and heavy ions

that are not fully ionized by the laser-induced fields. For the laser intensities assumed in the simulations, tunnel ionization is the dominant mechanism of ionization of the considered atoms. For all ionization levels of these atoms, the Keldysh parameter is much smaller than 1 and the ionization energies are considerably smaller than the electron rest energy (Popov, 2004; Kramida *et al.*, 2018). Under such conditions, the process of ionization of the target atoms could be described using the Ammosov-Delone-Krainov formula (Ammosov *et al.*, 1986; Chen *et al.*, 2013), which was implemented to the numerical code.

The simulations were carried out for a 30 fs laser pulse with a wavelength of 0.8 μm and circular polarization, a peak intensity of 10^{23} W/cm², and a beam width [full width at half maximum (FWHM)] $d_L = 3 \mu\text{m}$ [these parameters correspond to a laser pulse energy of 220 J and are to be available at the ELI-Nuclear Physics infrastructure (Negoita *et al.*, 2016; <http://www.eli-laser.eu>)]. The laser beam shape in space (along the y -axis) and time was described by a super-Gaussian function with a power index equal to 6. The laser pulse interacted with a flat carbon, copper or lead target with a thickness (L_T) equal to 100 nm, a transverse size of 16 μm and an atom density corresponding to a solid-state density (1.76×10^{23} atoms/cm³ for carbon, 8.45×10^{22} atoms/cm³ for copper, and 3.30×10^{22} atoms/cm³ for lead). A pre-plasma with a density scale length of 20 nm and with a density shape described by an exponential function was placed in front of the target. The simulations were performed in the x, y space of dimensions $80 \times 20 \mu\text{m}^2$. The space and time steps were equal to 13.3 nm and 2.22 as, respectively. The number of ion macro-particles was assumed to be 4330800 (400 particles/cell) for C, 2165400 (200 particles/cell) for Cu and 1082700 (100 particles/cell) for Pb.

Ionizing properties of the generated ion beam

During the interaction of an ultra-intense laser beam with a solid target, the target atoms are ionized by a strong electric field of the laser beam. After the plasma has been produced, the ions created are additionally ionized by the strong electric field generated in the plasma as a result of the local imbalance between the positive charge of ions and the negative charge of the electrons surrounding the ions. In the considered case of ultra-relativistic laser intensities, the temperature of the plasma electrons is in the multi-MeV range (see further) and the electron mean free path is much longer than the target or the plasma size. As a result, the collisional ionization of the target atoms and the plasma ions by the electrons, as well as the electron-ion recombination, can be neglected.

Figure 1 presents the ionization spectra of ions, produced from the target made of C, Cu or Pb, at $t = 100$ fs, so at the late stage of the ion acceleration process ($t > 3\tau_L$, where τ_L is the laser pulse duration). The carbon target is ionized to the highest possible charge state $z = 6$ and actually, only one C ion specie with $z = 6$ is accelerated. In the case of a medium-heavy (Cu) or heavy (Pb) target, many highly charged ion species are produced and accelerated, and the mean ionization level in the ion beam is $Q_{\text{mean}} = 23.3$ for the Cu beam, and $Q_{\text{mean}} = 53.3$ for the Pb beam.

Figure 2 shows 2D spatial distributions of the ionization level in the ion beams generated from a C, Cu or Pb target at the late stage of ion acceleration. In the case of the C target, only ions with the charge state $z = 6$ occur both in the laser-irradiated and non-irradiated part of the target. In the beams of Cu and Pb ions, the spatial distribution of the ionization level is strongly inhomogeneous, with the highest ionization levels being observed in the

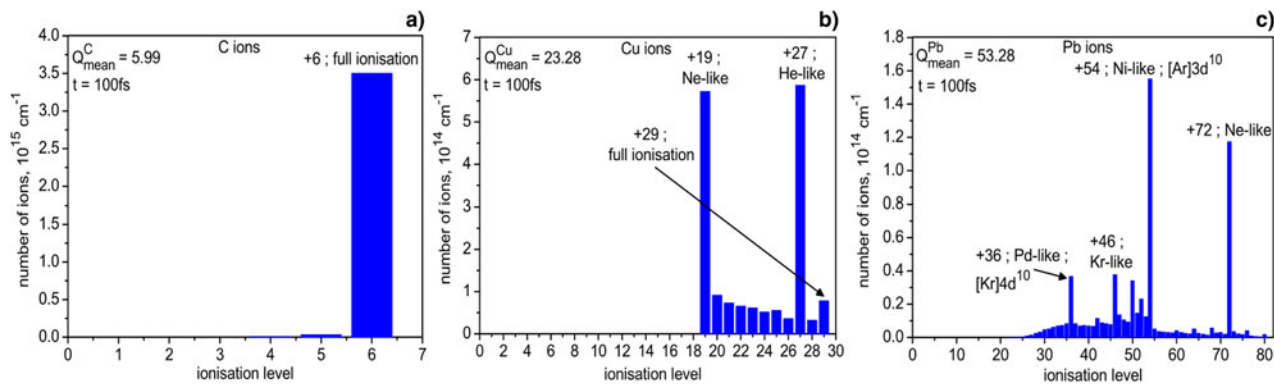


Fig. 1. The ionization spectra of ions produced from the target made of carbon (a), copper (b) or lead (c) at the late stage of ion acceleration.

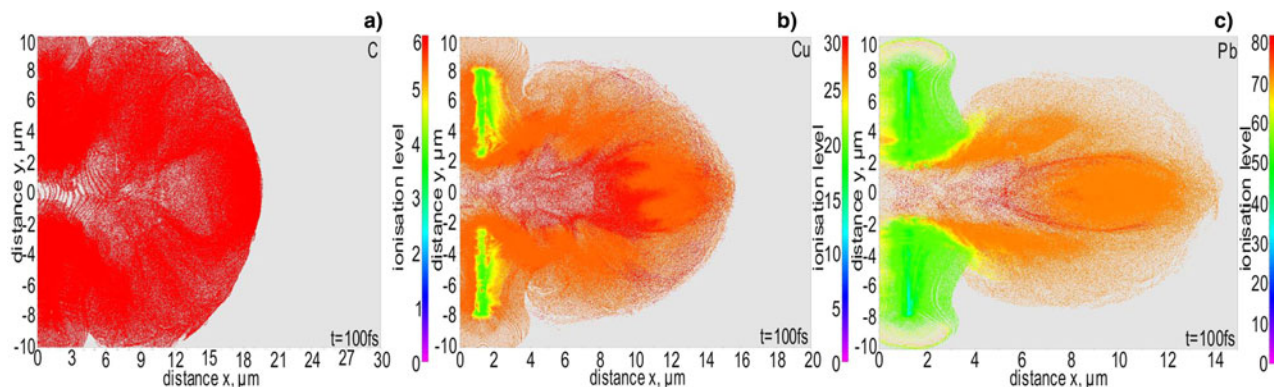


Fig. 2. 2D spatial distributions of the ionization level in the ion beams generated from the target made of carbon (a), copper (b) or lead (c) at the late stage of ion acceleration.

central part of the beam. It is worth emphasizing that both the ionization spectrum and the spatial distribution of the ionization level in the beam change during the acceleration process. This causes the ion acceleration process to be complex, especially in the case of acceleration of medium-heavy and heavy ions.

Spatial characteristics of the ion beam and ion acceleration mechanisms

Both the spatial distribution of the density of ions and electrons in the generated ion beam, as well as the distributions of laser-induced electric fields in the plasma are an important source of information on ion acceleration mechanisms. Understanding these mechanisms is, in turn, crucial for developing methods to control the ion acceleration process and obtain parameters of the ion beam desirable for specific applications. Figure 3 presents 2D spatial profiles of the ion density (a, d), electron density (b, e), and the electric field accelerating ions E_x (c, f) at the early stage ($t \sim \tau_L$) of the acceleration process for the C and Pb targets. At this stage, RPA is a dominant acceleration mechanism both for light and heavy ions, and in both cases, fairly dense and compact ion (plasma) bunches are accelerated along the laser beam axis. The ion densities in the bunches approach the densities of the solid targets from which the bunches are produced, and the accelerating fields reach extremely high values ~ 1 TV/cm.

2D spatial profiles of the ion density (a, d), electron density (b, e), and the electric field accelerating ions E_x (c, f) at the late stage ($t > 3\tau_L$) of ion acceleration are presented in Figure 4. At

this stage, both light and heavy ions are accelerated by an electric field created by hot electrons moving far away from the ions. This field is strong enough (the field amplitude locally surpasses 100 GV/cm) not only to effectively accelerate the ions from the central region of the target irradiated by the laser beam but also to ionize the target atoms and accelerate the formed ions from the non-irradiated part of the target. This sheath acceleration (SA) mechanism results in a rather complex structure of the ion beam, though also in this case a relatively dense and compact ion (plasma) bunch accelerated along the laser beam axis can be observed. The ion acceleration mechanisms are even more clearly visible in Figure 5, where the spatial profiles of the ion density, the electron density, and the electric field accelerating ions E_x along the laser beam axis at the early (a,c) and late (b, d) stages of ion acceleration are shown. At the early stage, the RPA field clearly prevails over the SA field for both light and heavy ions. At the late stage, the ions are accelerated by the SA field, which is significantly weaker than the RPA field, however. As a result, most of the energy was delivered to the ion beam in the RPA stage. At the late stage of acceleration, some differences in the acceleration mechanisms of light and heavy ions can be observed. In the case of light ions, the Coulomb explosion of ions affects the acceleration process, while in the case of heavy ions this effect does not occur. The main reason for this seems to be the strong compression of the carbon plasma bunch in the RPA acceleration stage, which causes the electrons surrounding the carbons ions to be unable to shield the ions efficiently enough in the post-RPA stage when the radiation pressure that compressed the bunch is equal to zero.

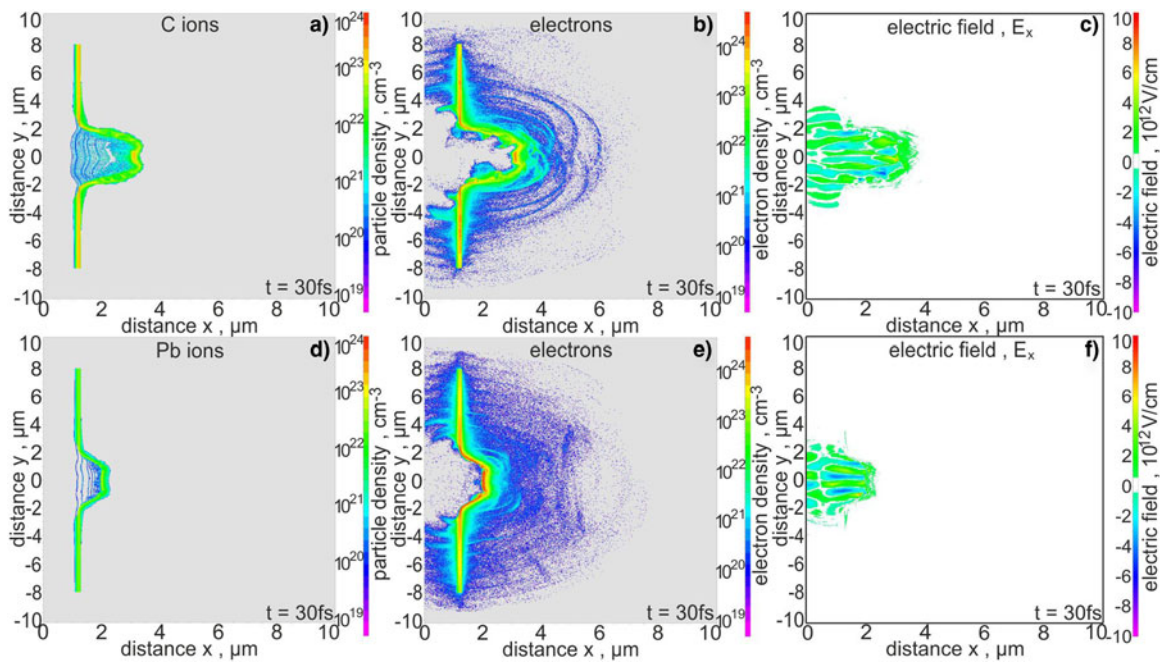


Fig. 3. 2D spatial distributions of the ion density (a, d), electron density (b, e), and the electric field accelerating ions E_x (c, f) at the early stage of ion acceleration for the carbon (a, b, c) and lead (d, e, f) targets.

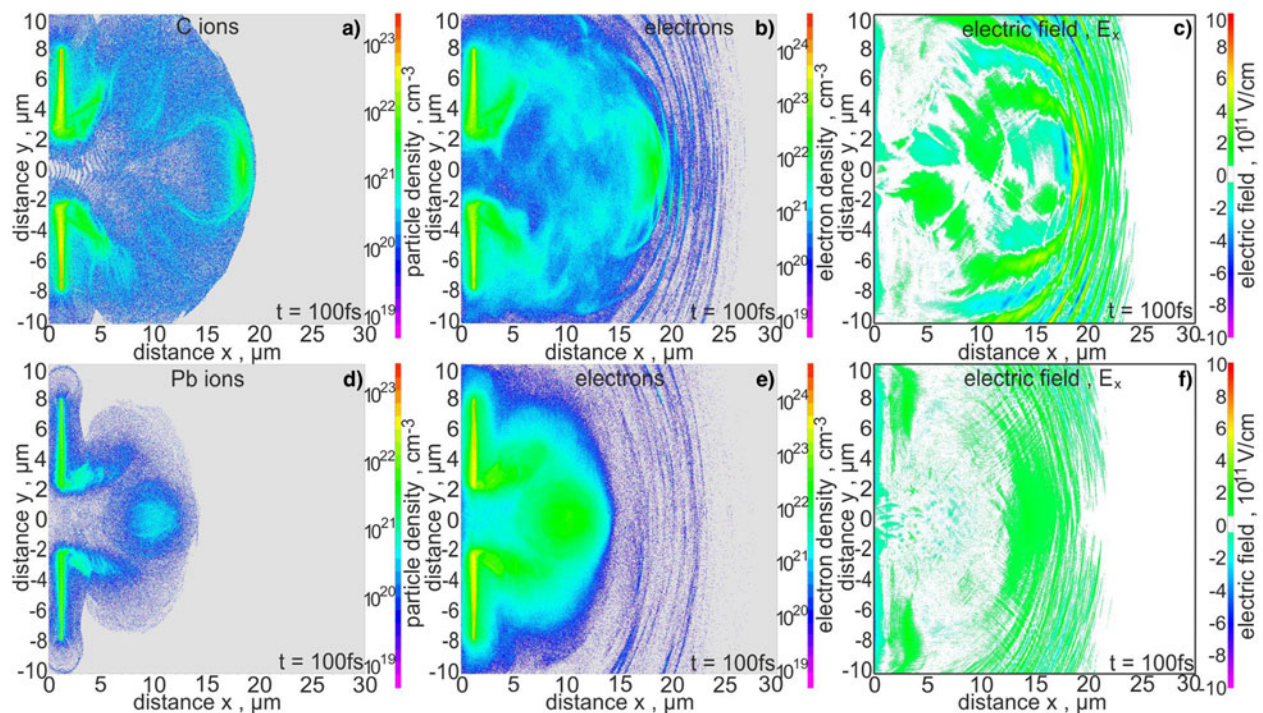


Fig. 4. 2D spatial distributions of the ion density (a, d), electron density (b, e), and the electric field accelerating ions E_x (c, f) at the late stage of ion acceleration for the carbon (a, b, c), and lead (d, e, f) targets.

The ion energy spectra

The energy spectra of C, Cu, and Pb ions for the central (“useful”) part of the ion beam of diameter $d_C = 2d_L = 6 \mu\text{m}$ and for the final stage of ion acceleration ($t = 250 \text{ fs}$) are shown in Figure 6. For a better visualization of the structure of these spectra, they were

presented using both the logarithmic scale and linear scale on the vertical axis. For all the ion beams considered, the spectra are broad, though their shapes are different. In the case of C and Cu ions, the two-peak structure in the high-energy range of the spectrum is clearly visible, while in the case of Pb ions,

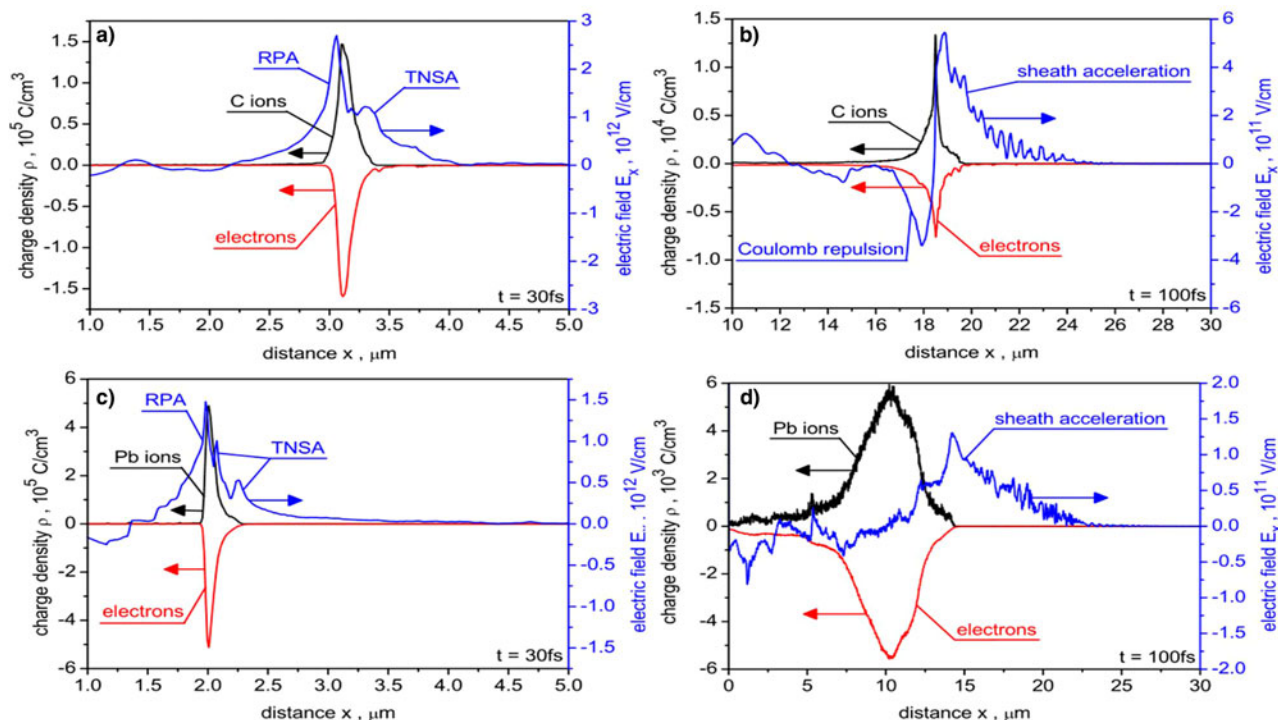


Fig. 5. Spatial profiles of the ion density, the electron density and the electric field accelerating ions, E_x , along the laser beam axis in the carbon (a, b) and lead (c, d) ion beams at the early (a, c) and late (b, d) stages of ion acceleration.

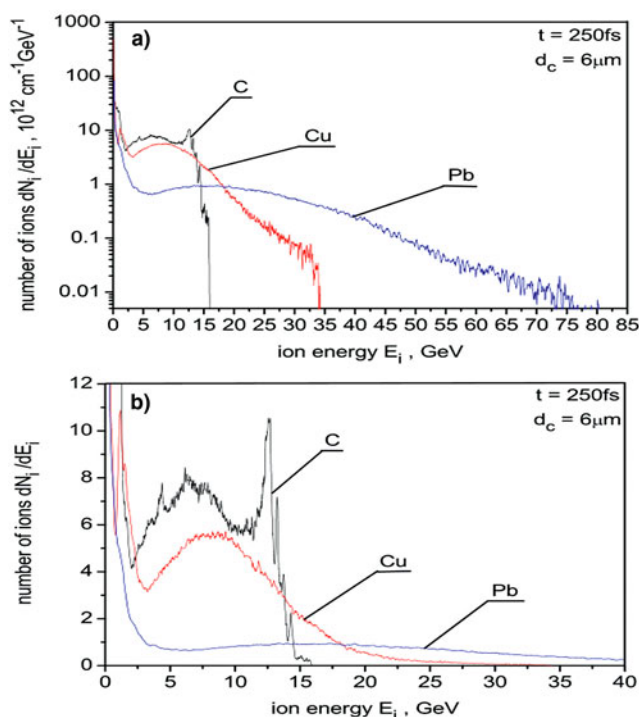


Fig. 6. The energy spectra of C, Cu, and Pb ions for the central part of the ion beam with a diameter of $d_c = 6\mu\text{m}$ presented using the logarithmic scale (a) and the linear scale (b) on the vertical axis.

only a very flat and wide peak in the energy spectrum can be seen. In general, the complex structure of the spectra is a reflection of the complex spatial structure of the ion beam (see Fig. 4) and

the contribution of the RPA and SA mechanisms to the ion acceleration process. In the case of medium-heavy (Cu) and heavy (Pb) ions, the main reason for the wide energy spectrum of these ions is the presence of many ion species with different q_i/m_i ratios in the ion beam (q_i is the ion charge and m_i is the ion mass), which results in different acceleration efficiencies of these ion species. In the case of the carbon ion beam, only one type of ion with $z=6$ is actually accelerated, though there is an additional factor causing the broadening of the spectrum, namely the Coulomb explosion in the SA dominated acceleration stage. An additional factor causing the broadening of the spectrum that occurs in all the considered cases is the heterogeneity of the transverse distribution of the intensity in the laser beam.

The absolute values of the maximum and mean energy of C, Cu, and Pb ions, as well as the ion energies per nucleon, calculated for the central part of the ion beam of $d_c = 6\mu\text{m}$, are presented in the diagram in Fig. 7. The absolute values of the ion energies grow with the increase of the ion mass (the ion mass number) while the ion energies per nucleon decrease with the increase of the ion mass. The main reason for this decrease is a decrease in the average value of the q_i/m_i ratio in the ion beam with the growth in the ion mass, which the values for C, Cu, and Pb ions are equal to 0.5, 0.37, and 0.26, respectively. For all kinds of ions considered, the mean ion energies are in the multi-GeV range and the maximum energies reach into the tens of GeV.

The number of accelerated ions and the laser-to-ions energy conversion efficiency

The total number of accelerated C, Cu, and Pb ions, and the number of high-energy ($E_i > 1\text{ GeV}$) ions for the central region of the ion beam ($d_c = 6\mu\text{m}$) and for the whole beam, is shown in

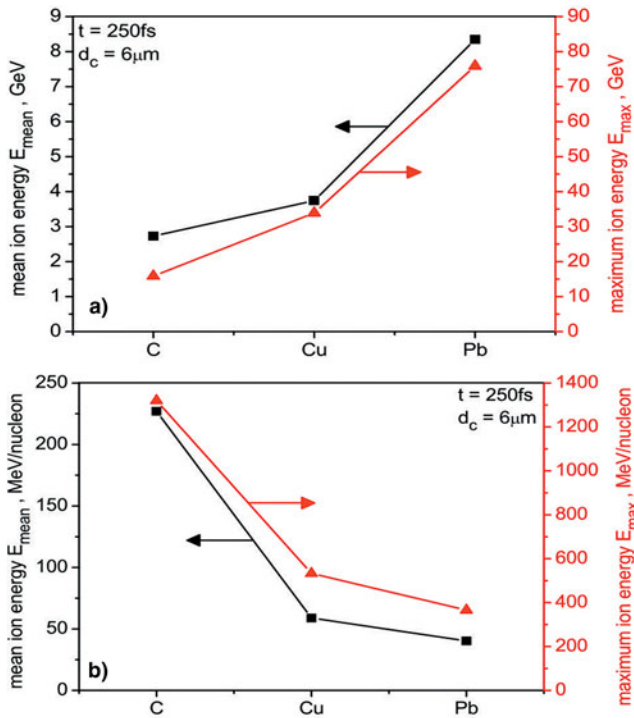


Fig. 7. The absolute values of the maximum and mean energy of C, Cu, and Pb ions (a) and the ion energies per nucleon (b), calculated for the central part of the ion beam with $d_c = 6 \mu\text{m}$.

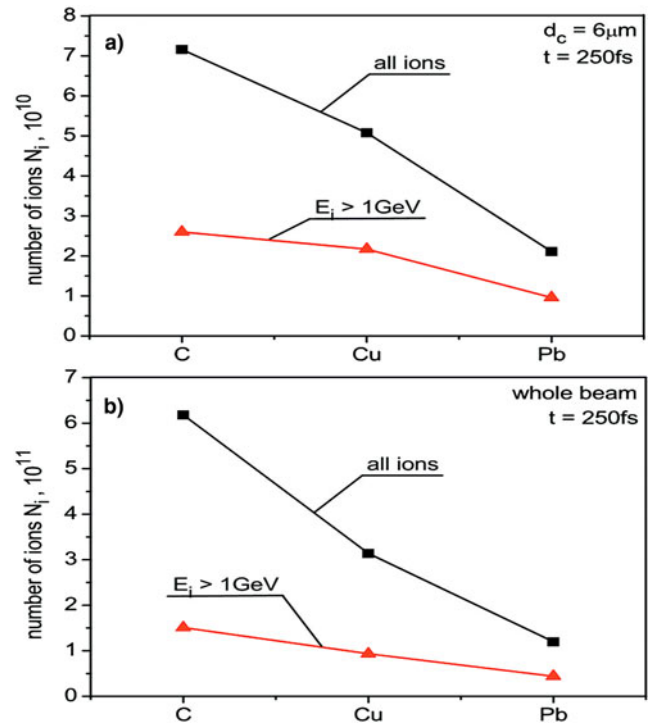


Fig. 8. The total number of accelerated C, Cu, and Pb ions and the number of high-energy ($E_i > 1\text{GeV}$) ions for the central region of the ion beam with $d_c = 6 \mu\text{m}$ (a) and for the whole beam (b).

Figure 8. In turn, Figure 9 presents the laser-to-ions energy conversion efficiency for all the ions and the high-energy ions for the beam central region and for the whole beam. Both the number of accelerated ions and the laser-to-ions energy conversion efficiency decrease with an increase in the ion mass, though the decrease in the conversion efficiency is much smaller, as the energies of heavy ions are significantly higher than those of the light ions (Fig. 7). It can also be seen that most of the energy of the ion beam is concentrated in high-energy ions with GeV energies and the conversion efficiency is fairly high – above 10% for the central region and above 30% for the whole beam. It is significant that the energy accumulated in the whole beam is about three times higher than the energy contained in its central, most intense part, driven mainly by the RPA mechanism. This is due to the fact that, although the ions from outside the central region are less energetic, their number is nearly an order of magnitude higher than in the central region, and as a result, they carry most of the energy stored in the beam. This, in turn, means that most of the laser energy is transferred to the ion beam via an accelerating field created by hot electrons pushed out of the central region by laser-induced ponderomotive forces (see Fig. 4).

The ion beam fluence, intensity, and duration

Important parameters of ultra-intense ion beams are the ion fluence F_i (the number of ions per cm^2), the ion energy fluence F_{ie} (measured in J/cm^2), and the beam peak intensity I_i (measured in W/cm^2), as well as the ion pulse duration and shape. Figure 10 presents the ion fluence and the ion energy fluence of the C, Cu, and Pb ion beams for all ions generated from the central region of the target ($d_c = 6 \mu\text{m}$), as well as the F_i and F_{ie} values for the high-energy ions with $E_i > 1\text{GeV}$. The ion fluence decreases

with an increase in the ion mass, while the ion energy fluence of the beam is almost independent of the ion mass since the reduction in the number of ions is compensated by the increase in their energy. Both the ion fluence and the ion energy fluence reach very high values ($F_i > 10^{17}$ ions/ cm^2 , $F_{ie} > 10^8$ J/ cm^2) hardly achievable in conventional RF-driven accelerators.

The temporal shape, peak intensity, and duration of the ion pulse generated from the target made of C, Cu, or Pb and recorded at the distance of $30 \mu\text{m}$ behind the target, are shown in Figures 11 and 12. It can be seen that the peak intensity of the ion pulse decreases and the pulse duration increases, with an increase in the ion mass. Although the energy spectra of accelerated ions are broad, the ion pulse durations are very short, $\sim 10\text{--}60$ fs, since the spatial length of the main, most energetic ion bunch in the C, Cu or Pb ion beam is only a few μm , and the mean velocity of the bunch is very high $> 10^{10}$ cm/s. Peak intensities of the ion pulses reach extremely high values $\sim 10^{21}\text{--}10^{22}$ W/ cm^2 because the ion bunches are dense and the ions in the bunch have high velocities and energies (the ion pulse intensity $I_i = n_i v_i E_i$, where n_i , v_i , and E_i are the ion density, velocity and energy, respectively). The demonstrated values of the ion pulse duration are by a factor of $10^4\text{--}10^5$ shorter, and the peak intensities are by a factor of 10^2 higher than those attainable currently in conventional RF-driven ion accelerators. Also, peak powers of the ion pulses are very high and at the distance of $30 \mu\text{m}$ behind the target they reach values about 2.5 PW for the C ion beam, 0.5 PW for the Cu beam, and 0.4 PW for the Pb beam.

The angular divergence of the ion beam

Significant inhomogeneity of the charge density distribution in the ion beam (especially pronounced in the case of the Pb and

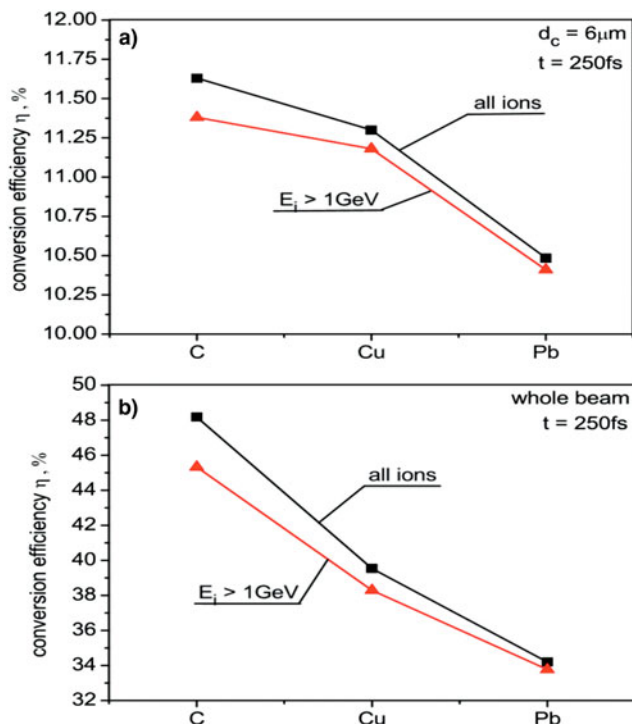


Fig. 9. The laser-to-ions energy conversion efficiency for all the ions and the high energy ($E_i > 1\text{GeV}$) ions for the central region of the ion beam with $d_c = 6 \mu\text{m}$ (a) and for the whole beam (b).

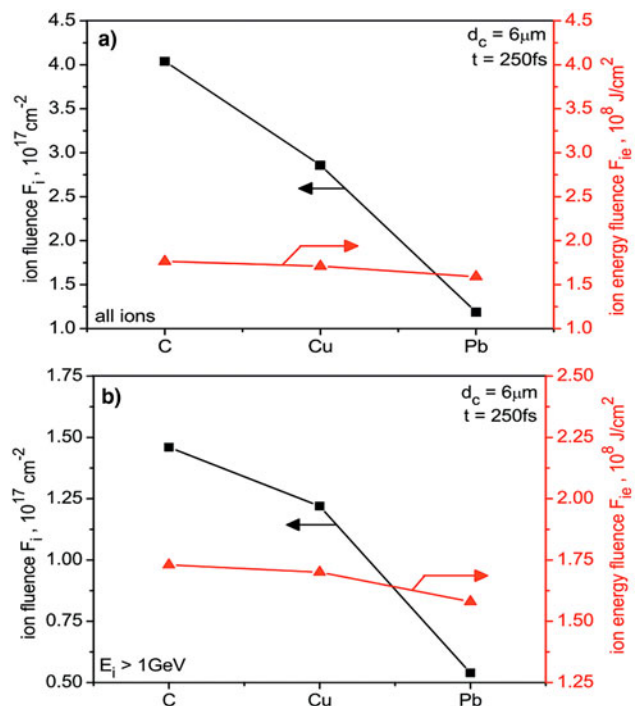


Fig. 10. The ion fluence and the ion energy fluence for all the ions (a) and the high energy ions (b) accelerated in the central region of the C, Cu, and Pb beams.

Cu ion beams – Fig. 2) and the complex and non-uniform structure of the field accelerating ions in the post-RPA stage (Fig. 4) result in the distribution of ion velocities in the beam, in both axial and radial directions, also being inhomogeneous, and therefore the angular distribution of the beam intensity is fairly complex, with the effective angular divergence of the beam being significant. This is illustrated in Figure 13, where the angular distribution of beam intensity in the x - y plane and the effective (FWHM) angular divergence of the C, Cu, and Pb ion beams is shown. It can be seen that the angular distribution of the beam intensity essentially depends on the type of accelerated ions, and the angular divergence of the light ion beam is half the value of the angular divergence of medium-heavy and heavy ion beams. One of the reasons for this is the better uniformity of the charge density distribution in the light ion beam (Fig. 2). A relatively large angular divergence of the ion beam and the dispersion of the ions velocity cause that the intensity of the beam decreases quite rapidly with the increase of the distance from the laser-irradiated target, and achieving a high intensity of the ion beam is possible only at small (sub-millimetre) distances from the target. Thus, in ion beam–target interaction experiments in which a high ion beam intensity is desired, the distance between the laser-irradiated target and the beam-irradiated target should be as small as possible.

The influence of radiation losses and other effects on the parameters of ultra-intense ion beams

Laser-driven ion acceleration at ultra-relativistic laser intensities can potentially be accompanied by the generation of ultra-relativistic electrons with the Lorentz factor $\gamma \gg 1$ (electron

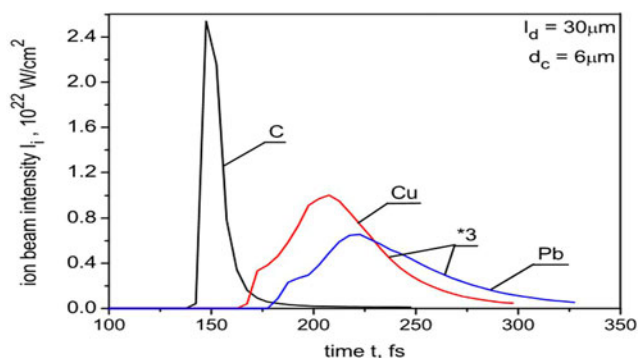


Fig. 11. The temporal shapes of ion pulses generated from the central region ($d_c = 6 \mu\text{m}$) of the carbon, copper or lead target recorded $30 \mu\text{m}$ behind the target.

energies of tens of MeV or higher), which can lose part of their energy due to synchrotron radiation, and these radiation losses (RL) can influence the ion acceleration process (e.g. Capdessus and McKenna, 2015; Tamburini *et al.*, 2010). It was shown, for example in Capdessus and McKenna (2015), that the RL of ultra-relativistic electrons can significantly affect the acceleration of protons or deuterons driven by a laser pulse with an intensity of 10^{23}W/cm^2 , and can enhance or reduce the ion acceleration efficiency in dependence on the target areal density. However, as it was shown in Tamburini *et al.* (2010), the influence of RL on ion beam parameters significantly depends on the laser beam polarization, and for the circular polarization this influence can be small, even at very high laser intensities $\sim 10^{24} \text{W/cm}^2$. In general, the influence of RL on the ion acceleration process depends on both the laser pulse and target parameters, and can significantly affect this

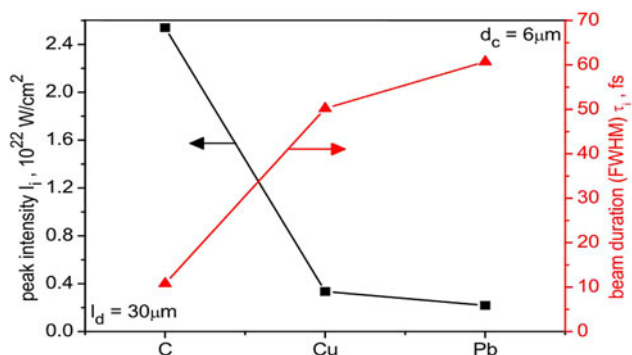


Fig. 12. The peak intensity and duration of ion pulses generated from the central region ($d_c = 6 \mu\text{m}$) of the carbon, copper or lead target recorded $30 \mu\text{m}$ behind the target.

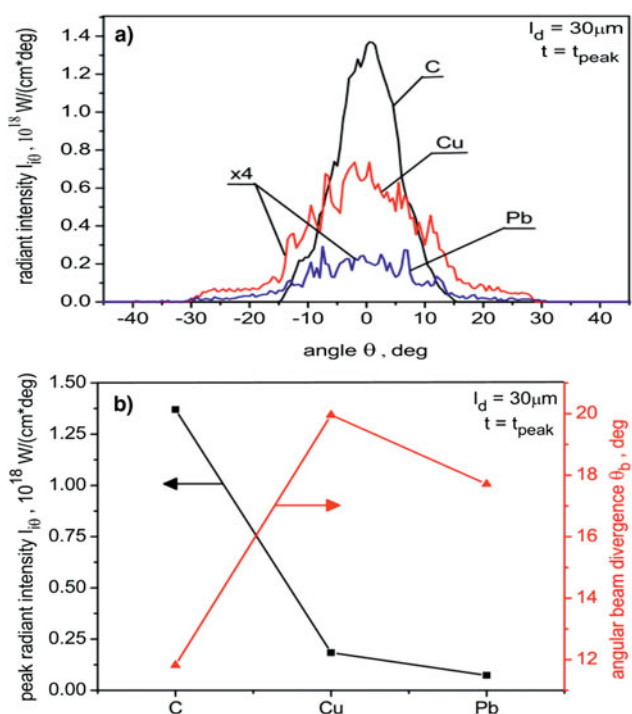


Fig. 13. The angular distribution of beam intensity in the x - y plane (a) as well as the peak intensity and the angular divergence (b) of the C, Cu, and Pb ion beams in this plane recorded in the maximum of the ion pulse at a distance of $30 \mu\text{m}$ behind the target.

process only if certain specific laser–target interaction conditions are met.

In order to check the possible influence of RL on the parameters of ultra-intense ion beams considered in this paper, we analyzed the energy spectra of electrons generated from C, Cu or Pb targets during the ion acceleration process. Figure 14 presents the energy spectra of fast electrons generated from the C, Cu, and Pb targets. In the case of medium-heavy (Cu) and heavy (Pb) targets, the mean electron energies are relatively small (2.6 MeV and 2.5 MeV, respectively) and the energy stored in ultra-relativistic electrons (of energy $>50 \text{ MeV}$) is below 1% of the total electron energy. There are two reasons for such a small contribution of ultra-relativistic electrons in the electron energy balance. The first reason is the strong coupling of the vast majority of electrons

with ions (Figs 3 and 4), resulting from the high charge state of Cu and Pb ions (Fig. 1), and the relatively small, non-relativistic mean velocities of these ions. The second reason is the circular polarization of the laser beam, which is much less effective in producing high-energy electrons than linear polarization (Macchi *et al.*, 2005; 2013; Zheng *et al.*, 2012). Because the source of RL is ultra-relativistic electrons, the small total energy stored in these electrons means that a total energy loss due to synchrotron radiation is also small, so the effect of RL on parameters of the Cu and Pb ion beams should be negligible. The electrons generated from the light (C) target are more energetic than those generated from the heavier targets – the mean energies of these electrons are equal to about 12 MeV, and the energy stored in the ultra-relativistic electrons reaches several per cent of the total electron energy. Probable reasons for the observed differences between energies of electrons generated from the light and heavy targets are the smaller charge state of C ions and their higher velocities. Thus, in the case of the C target, the RL can be noticeable, and the effect of RL on the C ion energy spectrum, especially the maximum energy of C ions, can be noticeable as well. However, the effect of RL on the most important parameters of ultra-intense C ion beams, such as the beam intensity and fluence, the ion pulse duration, the ion bunch density and velocity is expected to be small, as in the case of Cu and Pb ion beams.

Another possible source of energy loss of accelerated ions, which was not taken into account in our investigations of ultra-intense ion beam generation, are hydrocarbon contaminants, usually occurring on the surfaces of solid targets, especially on metal targets. The protons from contaminants are accelerated by the sheath field created by hot electrons and when SA is a dominant mechanism of ion acceleration, the energy carried by protons can significantly decrease the laser energy converted to heavier ions. However, in the cases considered in our paper, most of the energy is delivered to the ion beam by the RPA mechanism (see the section Spatial characteristics of the ion beam and ion acceleration mechanisms), and especially the parameters of the dense ion bunch formed by RPA and accelerated along the laser beam axis are expected to be weakly influenced by proton contaminants. Since the parameters of this ion bunch determine the most important parameters of the ultra-intense ion pulse (the ion pulse fluence, intensity, duration, and mean energy), the effect of energy losses associated with the existence of contaminants on the ion pulse parameters is expected to be small. The influence of these losses on parameters of the heavy (thorium) ion beam driven by a femtosecond laser pulse with intensity 10^{23} W/cm^2 was checked in (Domański and Badziak, 2018), where the PIC simulation of heavy ion generation from the 100 nm thorium target with the proton layer of a thickness of 26.6 nm and a density equal to 0.1 g/cm^3 , situated inside the target close to the target rear surface, was performed. The simulations showed a decrease in the maximum energy of heavy ions equal to 9%, and a negligible influence of the proton layer on the mean ion energy, intensity, and duration of the heavy ion beam. Since the laser and target parameters in this simulation were similar to those in our present work, it is reasonable to believe that the effect of hydrocarbon contaminants on parameters of ultra-intense ion beams investigated in this work will be small, at least in the case of Pb and Cu ion beams.

Therefore, we have reasons to believe that, in the cases considered in this paper, the impact of both radiation energy losses due to synchrotron radiation and energy losses resulting from the presence of hydrocarbon contaminants in the target on ion

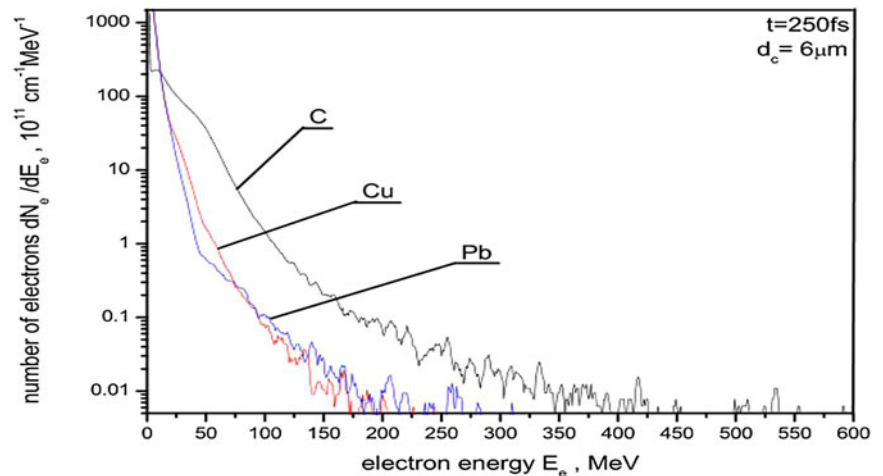


Fig. 14. The energy spectra of electrons generated from the central region ($d_c = 6 \mu\text{m}$) of the carbon, copper or lead target.

beam parameters of importance for potential applications of ultra-intense ion beams will be small.

Potential applications of ultra-intense laser-driven ion beams and research challenges

Ultra-intense ion beams have the potential to be applied in HED physics, nuclear physics, ICF and, possibly, in other research fields. A few examples of the potential applications are very briefly described below.

HED physics

The HED state of matter is usually defined as a state in which the energy density is $>10^5 \text{ J/cm}^3$ or, equivalently, the pressure is $>1 \text{ Mbar}$ (Drake, 2006). The creation and examination of such states of matter are desirable for research in materials science, astrophysics, planetology, and ICF. HED states are routinely produced by high explosives, pulsed-power (Z-pinch) devices, high-peak-power lasers and intense particle beams (Drake, 2006; Hoffmann *et al.*, 2009; Sharkov *et al.*, 2016). Particle beams, and especially ion beams, have a number of advantages in the creation of HED states, in particular: The possibility of deep penetration into the target; the ability to create HED states in practically any dense material; and the relatively good uniformity of the distribution of energy deposited in the material.

The key parameters characterizing an ion beam's ability to create HED states are the energy deposited per gram of matter (Sharkov *et al.*, 2016): $E_s = (1.6 \times 10^{-19})(dE_i/dx)F_i$ [J/g] and the deposition power $P_s = E_s/t_d$, where dE_i/dx is the ion stopping power of the material, F_i is the ion fluence and t_d is the energy deposition time. To assess this ability for the ion beams considered in this paper, let us estimate the values of E_s and P_s for the case of the interaction of the Pb ion beam accelerated by the multi-PW laser considered in the paper with a carbon target. For a very rough estimate of these values, we assume that the stopping power for the laser-driven ions characterized by the mean ion energy is similar to the stopping power of ions with the same mean energy produced in a conventional accelerator. Taking into account the Pb ion beam parameters: The mean ion energy $\langle E_i \rangle \approx 40 \text{ MeV/nucleon}$, $F_i \approx 1.2 \times 10^{17} \text{ cm}^{-2}$, $\tau_i \approx 60 \text{ fs}$ (see Figs 7, 10 and 12), the stopping power for 40-MeV Pb ions in carbon $dE_i/dx \approx 60 \text{ MeV/(mg/cm}^2)$ (Paul, 2012) and

assuming $t_d \approx \tau_i$, we obtain: $E_s \approx 1.2 \text{ GJ/g}$, $P_s \approx 2 \times 10^{22} \text{ W/g}$. For a comparison, the E_s and P_s values predicted for heavy ion beams produced by very big RF-driven heavy ion accelerators, such as the Facility for Antiproton and Ion Research (FAIR) accelerator (being built in GSI, Darmstadt) or the High Intensity heavy ion Accelerator Facility (HIAF) accelerator (designed in the Institute of Modern Physics, Lanzhou), approach $\sim 0.1 \text{ MJ/g}$ and $\sim 10^{12} \text{ W/g}$ for FAIR and $\sim 1 \text{ MJ/g}$ and 10^{13} W/g for HIAF (assuming $t_d \sim \tau_i \sim 100 \text{ ns}$), respectively (Sharkov *et al.*, 2016). Thus, the values E_s and P_s estimated for the heavy ion beam driven by a multi-PW laser are by many orders of magnitude higher than those achievable for the biggest RF-driven accelerators. It should be emphasized, however, that the stopping power values for beams of such high intensities and densities as demonstrated in our work are, in fact, unknown, and the collective effects expected at such high ion beam densities can significantly modify the values predicted by the Bethe-Bloch equation and used for the above estimates. In addition to the very high intensities/fluencies and densities of ultra-intense ion beams driven by a multi-PW laser, an important parameter determining the interaction of such a beam with matter is the very short (sub-picosecond) duration of the beam. This means that the time of depositing energy in the material is much shorter than the time period in which the material parameters change due to its hydrodynamic motion and we deal with the isochoric heating of the material. Such an isochoric regime of beam-target interaction is hardly achievable with ion beams produced by RF-driven accelerators due to long (ns or longer) durations of these beams. Thus, the unique parameters of ultra-intense laser-driven ion beams make it possible to explore essentially new regimes of ion beam-matter interaction, not attainable or barely attainable for conventional accelerators.

Nuclear physics

The extremely high intensities and very short durations of ion beams driven by a multi-PW laser render nuclear physics research possible with unusual efficiency of the ion beam-target interaction and in principally new time scales. As a result, some low-cross-section and/or transient nuclear reactions that would be hardly observable using ion beams produced by a conventional RF-driven accelerator could be feasible to be investigated. Examples are the nuclear phenomena planned to be studied

within the research programme of the ELI-Nuclear Physics infrastructure. One of the topics in this program, which is particularly important for understanding the nature of the creation of heavy elements in the universe, is to study the production of neutron-rich heavy nuclei by a reaction mechanism called fission–fusion, using thorium (Th) ions accelerated by a multi-PW laser (Negoita *et al.*, 2016). The creation of a sufficiently large, measurable amount of the neutron-rich heavy nuclei in this way requires, however, thorium ion beams with very high ion fluencies F_i and beam intensities I_i that are unachievable in RF-driven accelerators. In particular, the ion beam parameters should be as follows: A mean energy of thorium ions of 1.6 GeV, $F_i \sim 10^{18} \text{ cm}^{-2}$, $I_i \sim 10^{20} \text{ W/cm}^2$ and the total number of thorium ions $N_i \sim 10^{11}$ (Negoita *et al.*, 2016). Our numerical investigation into the acceleration of lead ions presented above (the atomic numbers and masses of Pb and Th ions are very similar), as well as the studies presented in (Domański and Badziak, 2018), showed that these ion beam parameters are within the reach of a laser accelerator of heavy ions driven by the ELI-NP multi-PW laser.

Inertial confinement fusion

An important potential application of ultra-intense ion beams is ICF. In the so-called fast ignition (FI) scenario of ICF, a deuterium–tritium (DT) fuel compressed by high-energy ns laser or X-ray beams is ignited by an ultra-intense particle (electron or ion) beam (Fernandez *et al.*, 2014). The FI approach has substantial advantages over conventional, central-hot-spot ICF, in particular: Higher energy gain, lower required driver energy, lower susceptibility to hydrodynamic instabilities and flexibility in using different compression drivers. In the case of using light or moderate-heavy ion beams for high-gain DT fusion in the FI approach, the required parameters of the ion beam are estimated to be as follows (Davis *et al.*, 2011; Fernandez *et al.*, 2014): The mean ion energy ~ 10 – 50 MeV/nucleon , the beam intensity $\sim 10^{20} \text{ W/cm}^2$, the ion pulse duration $\sim \text{ps}$, and a total beam energy of ~ 10 – 20 kJ . Although the required beam energy is attainable only using 100 kJ-class short-pulse laser drivers, the remaining beam parameters are well within the reach of multi-PW laser drivers such as ELI lasers. As demonstrated above, the mean ion energies and beam intensities of the ion beams driven by the multi-PW ELI laser can be significantly higher and the beam duration can be much shorter than required. Moreover, the last two parameters can be simply controlled by changing the distance between the ion source and the ion beam-irradiated target. Thus, these beams can be quite effectively applied in various areas of fundamental research into the FI approach to ICF.

Research challenges

Although extremely high intensities/fluencies and very short durations of multi-PW laser-driven ion beams demonstrated in our paper promise unique applications of these beams in various scientific domains, in order to make these applications reality, other parameters of the beams should be improved and the beam characteristics must be controlled and matched to the type of application envisaged.

For the application of ultra-intense laser-driven ion beams in nuclear physics, the ion energy spectrum width should be decreased and the ion energies should be controlled and adjusted to the requirements of a particular experiment. A significant narrowing of the ion energy spectrum (down to just a few percent)

would create a chance to use light ion beams such as the carbon beam for medical applications, in particular for hadron cancer therapy. Both for applications in nuclear physics and medicine, it is desirable that the ion beams are generated with a high repetition rate (several Hz or higher) which is a significant challenge for multi-PW laser technology. Moreover, since in the above applications, especially in hadron therapy, the ion beam must usually be transported over a relatively long distance, the angular beam divergence should be as small as possible. Applications of ultra-intense ion beams in HED physics or ICF research do not require very high ion energies or very narrow ion energy spectra, and ion energies from several MeV/nucleon to tens of MeV/nucleon and spectral widths of 10–20% of the mean ion energy are usually sufficient for these applications. In addition, a high repetition rate of a laser driver is not necessary in order to perform HEDP or ICF experiments. However, for “full-scale” FI ICF experiments, the required values of ion beam power and energy are extremely high, attainable only with 100 kJ-class laser drivers, which will probably not be available in the near future. Fortunately, as was mentioned previously, fundamental research in ICF with multi-PW laser-driven ion beams will be possible with currently built multi-PW lasers.

The majority of applications of laser-driven ion beams require compact and cost-effective laser accelerators. The size, cost, and complexity of the accelerator are determined first of all by the laser driver, in particular by energy of the laser pulse produced by the driver. The way to minimize this energy without a significant reduction in the ion beam parameters is to increase the laser-to-ions energy conversion efficiency. One of the main challenges in the study of laser-driven ion acceleration is to increase this efficiency to a level ensuring compactness and cost of the accelerator enabling its practical usefulness.

The usefulness of laser-driven ion beams in scientific research as well as in technology or medicine also depends on whether at least some parameters of these beams can be higher/better than or comparable to those achieved in RF-driven accelerators. It is very likely that, in the foreseeable future, energies of laser-accelerated ions will still be considerably lower than the highest energies of ions achieved in large RF-driven accelerators. Obtaining in laser accelerators very narrow ion energy spectra whose spectral widths are comparable to those achieved in conventional accelerators is also rather unlikely. On the other hand, as was demonstrated in this paper, achieving peak ion beam intensities, peak ion current densities or ion fluencies higher than attainable presently in the RF-driven accelerators is feasible with currently built multi-PW lasers, so it is conceivable that it will be experimentally demonstrated over the next few years.

Conclusions

In conclusion, the process of accelerating light (C), medium-heavy (Cu) and heavy (Pb) ions by a multi-PW laser pulse of ultra-relativistic intensity to be available at the ELI infrastructure has been investigated using an advanced PIC code. It has been found that, regardless of the ion mass, the RPA stage of ion acceleration is followed by the SA stage driven by the electric field created by fast electrons moving far away from the ions. However, the majority of the energy carried by the most energetic and intense (central) part of the beam comes from the RPA stage and is concentrated in a fairly compact and dense ion bunch. In the case of light ions, only one ion specie with the highest

possible charge state is actually produced and accelerated, while in the case of heavier ions, many highly charged ion species are accelerated, while the ionization level distribution in the ion beam is strongly inhomogeneous and changes over time. This fairly complex, hybrid mechanism of ion acceleration at ultra-relativistic laser intensities leads to the production of a high-energy (multi-GeV) ion beam with a broad energy spectrum. Both the mean and the maximum ion energies in the beam, as well as the ion beam duration, grow with the increase of the ion mass, while the ion energies per nucleon, the ion beam intensities, and the ion fluencies decrease with increasing ion mass.

It has been shown that a 220-J, 30-fs laser pulse with an intensity of 10^{23} W/cm² irradiating a 0.1- μ m solid target made of C, Cu or Pb is capable of producing, with a high (>10%) laser-to-ions energy conversion efficiency, multi-GeV ion beams with a petawatt peak power, ion fluence $\sim 10^{17}$ – 10^{18} ions/cm², peak intensity $\sim 10^{21}$ – 10^{22} W/cm², and time duration ~ 10 – 100 fs. The demonstrated beam intensities are higher by a factor of $\sim 10^2$, and ion pulse durations are shorter by a factor of $\sim 10^4$ – 10^5 than those attainable currently in the largest RF-driven accelerators.

The unique properties of ion beams driven by a multi-PW laser pulse of ultra-relativistic intensity, in particular very high intensities/fluencies and very short duration of the beams, create the prospect of a variety of applications of these beams in HED physics, ICF, new areas of nuclear physics, and perhaps in other domains. However, to make this prospect a reality, considerable progress in understanding and controlling the mechanisms of ion acceleration at ultra-high laser intensities as well as in the technology of short-pulse laser drivers is necessary.

Acknowledgments. This work was supported in part by the EUROfusion Consortium (the RoHGIFE project) and has received partial funding from the Euratom research and training programme 2014–2018 and 2019–2020 under grant agreement No 633053. The simulations were carried out with the support of the Interdisciplinary Center for Mathematical and Computational Modelling (ICM), University of Warsaw under grant no. G57-20.

References

- Allen M, Patel PK, MacKinnon A, Price D, Wilks S and Morse E (2004) Direct experimental evidence of back-surface ion acceleration from laser-irradiated gold foils. *Physical Review Letters* **93**, 265004-1-4.
- Ammosov MV, Delone NB and Krainov VP (1986) Tunnel ionization of complex atoms and of atomic ions in an alternating electromagnetic field. *Soviet Physics JETP* **64**, 1191.
- Badziak J (2007) Laser-driven generation of fast particles. *Opto-Electronics Review* **15**, 1.
- Badziak J, Parys P, Vankov AB, Wołowski J and Woryna E (2001) Generation of fluxes of highly charged ions from a picosecond laser-produced plasma. *Applied Physics Letters* **79**, 21–23.
- Badziak J, Głowacz S, Jabłoński S, Parys P, Wołowski J, Hora H, Krasa J, Laska L and Rochlena K (2004) Production of ultrahigh ion current densities at skin-layer subrelativistic laser–plasma interaction. *Plasma Physics and Controlled Fusion* **46**, B541–B555.
- Badziak J, Jabłoński S, Parys P, Rosiński M, Wołowski J, Szydłowski A, Antici P, Fuchs J and Mancic A (2008) Ultraintense proton beams from laser-induced skin-layer ponderomotive acceleration. *Journal of Applied Physics* **104**, 063310.
- Badziak J, Jabłoński S, Pisarczyk T, Rączka P, Krokusky E, Liska R, Kucharik M, Chodukowski T, Kalinowska Z, Parys P, Rosiński M, Borodziuk S and Ullschmied J (2012) Highly efficient accelerator of dense matter using laser-induced cavity pressure acceleration. *Physics of Plasmas* **19**, 053105.
- Badziak J, Parys P, Rosiński M, Krousky E, Ullschmied J and Torrisi L (2013) Improved generation of ion fluxes by a long pulse using laser-induced cavity pressure acceleration. *Applied Physics Letters* **103**, 124104.
- Borghesi M, Fuchs J, Bulanov SV, MacKinnon AJ, Patel PK and Roth M (2006) Fast ion generation by high-intensity laser irradiation of solid targets and applications. *Fusion Science and Technology* **49**, 412.
- Braenzel J, Andreev AA, Platonov K, Klingsporn M, Sandner W and Schnurer M (2015) Coulomb-Driven energy boost of heavy ions for laser-plasma acceleration. *Physical Review Letters* **114**, 124801.
- Bulanov SV, Esirkepov TZ, Khoroshkov VS, Kuznetsov AV and Pegoraro F (2002) Oncological hadrontherapy with laser ion accelerators. *Physics Letters A* **299**, 240–247.
- Bulanov SS, Esarey E, Schroeder CB, Bulanov SV, Esirkepov TZ, Kondo M and Leemans WP (2016) Radiation pressure acceleration: The factors limiting maximum attainable ion energy. *Physics of Plasmas* **23**, 056703.
- Bychenkov VY and Kovaliev VF (2005) Coulomb explosion in a cluster plasma. *Plasma Physics Reports* **31**, 178–183.
- Capdessus R and McKenna P (2015) Influence of radiation force on ultraintense laser-driven ion acceleration. *Physical Review E* **91**, 053105.
- Chen M, Cormier-Michel E, Geddes CGR, Bruhwiler DL, Yu LL, Esarey E, Schroeder CB and Leemans WP (2013) Numerical modelling of laser tunnelling ionization in explicit particle-in-cell codes. *Journal of Computational Physics* **236**, 220.
- Clark EL, Krushelnick K, Zepf M, Beg FN, Tatarakis M, Machacek A, Santala MIK, Watts I, Norreys PA and Dangor AE (2000) Energetic heavy-ion and proton generation from ultraintense laser-plasma interactions with solids. *Physical Review Letters* **85**, 1654–1657.
- Cowan TE, Fuchs J, Ruhl H, Kemp A, Audebert P, Roth M, Stephens R, Barton I, Blazevic A, Brambrink E, Fernandez J, Gauthier JC, Geissel M, Hegelich M, Kaee J, Karsch S, Le Sage GP, Letzring S, Manclossi M, Meyroneinc S, Newkirk A, Pepin H and Renard-LeGall-oudec N (2004) Ultralow emittance, multi-MeV proton beams from a laser virtual-cathode plasma accelerator. *Physical Review Letters* **92**, 204801–1–4.
- Daïdo H, Nishiuchi M and Pirozhkov AS (2012) Review of laser-driven ion sources and their applications. *Reports on Progress in Physics* **75**, 056401.
- Davis J, Petrov GM and Mehlhorn TA (2011) Generation of laser-driven light ions suitable for fast ignition of fusion targets. *Plasma Physics and Controlled Fusion* **53**, 045013.
- Domański J and Badziak J (2018) Ultra-intense femtosecond super-heavy ion beams driven by a multi-PW laser. *Physics Letters A* **382**, 3412–3417.
- Domański J, Badziak J and Jabłoński S (2017) Generation of proton beams from two-species targets irradiated by a femtosecond laser pulse of ultra-relativistic intensity. *Laser and Particle Beams* **35**, 286–293.
- Domański J, Badziak J and Marchwiany M (2018) Laser-driven acceleration of heavy ions at ultra-relativistic laser intensity. *Laser and Particle Beams* **36**, 507.
- Drake R.P. (2006). *High-Energy-Density Physics*, Berlin, Hidelberg: Springer-Verlag.
- Esirkepov T, Bingham R, Bulanov S, Honda T, Nishihara K and Pegoraro F (2000) Coulomb explosion of a cluster irradiated by a high intensity laser pulse. *Laser and Particle Beams* **18**, 503.
- Esirkepov T, Borghesi M, Bulanov SV, Mourou G and Tajima T (2004) Highly efficient relativistic-ion generation in the laser-piston regime. *Physical Review Letters* **92**, 175003.
- Fernandez JC, Albright BJ, Beg FN, Foord ME, Hegelich BM, Honrubia JJ, Roth M, Stephens RB and Yin L (2014) Fast ignition with laser-driven proton and ion beams. *Nuclear Fusion* **54**, 054006.
- Fritzer S, Malka V, Grillon G, Rousseau JP, Burgy F, Lefebvre E, d’Humieres E, McKenna P and Ledingham KWD (2003) Proton beams generated with high-intensity laser: applications to medical isotope production. *Applied Physics Letters* **83**, 3039–3041.
- Fuchs J, Antici P, d’Humie’res E, Lefebvre E, Borghesi M, Brambrink E, Cecchetti CA, Kaluza M, Malka V, Manclossi M, Meyroneinc S, Mora P, Schreiber J, Toncian T, Pepinand H and Audebert P (2006) Laser-driven proton scaling laws and new paths towards energy increase. *Nature Physics* **2**, 48–54.

- Głowacz S, Hora H, Badziak J, Jabłoński S, Cang Y and Osman F (2006) Analytical description of rippling effect and ion acceleration in plasma produced by a short laser pulse. *Laser and Particle Beams* **24**, 15–25.
- Grech M, Skupin S, Diaw A, Schlegel T and Tikhonchuk VT (2011) Energy distribution in radiation pressure accelerated ion beams. *New Journal of Physics* **13**, 123003.
- Higginson A, Gray RJ, King M, Dance RJ, Williamson SDR, Butler NMH, Wilson R, Capdessus R, Armstrong C, Green JS, Hawkes SJ, Martin P, Wei WQ, Mirfayzi SR, Yuan XH, Kar S, Borghesi M, Clarke RJ, Neely D and McKenna P (2018) Near-100 MeV protons via a laser-driven transparency-enhanced hybrid acceleration scheme. *Nature Communications* **9**, 724.
- Hoffmann DHH, Fortov VE, Kuster M, Mintsev V, Sharkov BY, Tahir NA, Udrea S, Varentsov D and Weyrich K (2009) High energy density physics generated by intense heavy ion beams. *Astrophysics and Space Science* **322**, 167.
- Jung D, Yin L, Albright BJ, Gautier DC, Hörlein R, Kiefer D, Henig A, Johnson R, Letzring S, Palaniyappan S, Shah R, Shimada T, Yan XQ, Bowers KJ, Tajima T, Fernández JC, Habs D and Hegelich BM (2011) Monoenergetic ion beam generation by driving ion solitary waves with circularly polarized laser light. *Physical Review Letters* **107**, 115002.
- Klimo O, Psikal J, Limpouch J and Tikhonchuk VT (2008) Monoenergetic ion beams from ultrathin foils irradiated by ultrahigh-contrast circularly polarized laser pulses. *Physical Review Special Topics – Accelerators and Beams* **11**, 031301.
- Koenig M, Benuzzi-Mounaix A, Ravasio A, Vinci T, Ozaki N, Lepape S, Batani D, Huser G, Hall T, Hicks D, MacKinnon A, Patel P, Park HS, Boehly T, Borghesi M, Kar S and Romagnani L (2005) Progress in the study of warm dense matter. *Plasma Physics and Controlled Fusion* **47**, B441–B449.
- Kramida A., Ralchenko Yu. and Reader J. & NIST ASD Team (2018). NIST atomic spectra database (ver. 5.5.2), Available at <http://physics.nist.gov/asd>, National Institute of Standards and Technology, Gaithersburg, MD, USA.
- Krushelnik K, Clark EL, Allot R, Beg FN, Danson CN and Machacek A (2000) Ultra-high intensity laser-produced plasmas as a compact heavy ion injection source. *IEEE Transactions on Plasma Science* **28**, 1184–1189.
- Ledingham KWD and Galster W (2010) Laser-driven particle and photon beams and some applications. *New Journal of Physics* **12**, 045005.
- Li J, Arefiev AV, Bulanov SS, Kawahito D, Bailly-Grandvaux M, Petrov GM, McGuffey C and Beg FN (2019) Ionization injection of highly-charged copper ions for laser-driven acceleration from ultra-thin foils. *Scientific Reports* **9**, 666.
- Macchi A, Cattani F, Liseykina TV and Cornalti F (2005) Laser acceleration of ion bunches at the front surface of over-dense plasmas. *Physical Review Letters* **94**, 165003.
- Macchi A, Borghesi M and Passoni M (2013) Ion acceleration by superintense laser-plasma interaction. *Reviews of Modern Physics* **85**, 751.
- MacKinnon AJ, Sentoku Y, Patel PK, Andersen C, Snavely R and Freeman RR (2002) Enhancement of proton acceleration by hot-electron recirculation in thin foils irradiated by ultraintense laser pulses. *Physical Review Letters* **88**, 215006-1-4.
- McKenna P, Ledingham KWD, Yang JM, Robson L, McCanny T, Shimizu S, Clarke RJ, Neely D, Spohr K, Chapman R, Singhal RP, Krushelnick K, Wei MS and Norreys PA (2004) Characterization of proton and heavier ion acceleration in ultrahigh-intensity laser interactions with heated target foils. *Physical Review E* **70**, 036405.
- Negoita F, Roth M, Thirolf PG, Tudisco S, Hannachi F, Moustazis S, Pomerantz I, McKenna P, Fuchs J, Spohr K, Acbas G, Anzalone A, Audebert P, Balascuta S, Cappuzzello F, Cernaianu MO, Chen S, Dancus I, Freeman R, Geissel H, Ghenuche P, Gizzi L, Gobet F, Gosselin G, Gugiu M, Higginson D, D’Humières E, Ivan C, Jaroszynski D, Kar S, Lamia L, Leca V, Neagu L, Lanzalone G, Meot V, Mirfayzi SR, Mitu IO, Morel P, Murphy C, Petcu C, Petrascu H, Petrone C, Racza P, Risca M, Rotaru F, Santos JJ, Schumacher D, Stutman D, Tarisien M, Tataru M, Tatulea B, Turcu ICE, Versteegen M, Ursescu D, Gales S and Zamfir NV (2016) Laser-driven nuclear physics at ELL_NP. *Romanian Reports in Physics* **68**, (Suppl.), S37–S144. <http://www.eli-laser.eu>.
- Nishiuchi M, Sakaki H, Esirkepov TZ, Nishio K, Pikuz TA, Faenov AY, Skobelev IY, Orlandi R, Sako H, Pirozhkov AS, Matsukawa K, Sagisaka A, Ogura K, Kanasaki M, Kiriya H, Fukuda Y, Koura H, Kando M, Yamauchi T, Watanabe Y, Bulanov SV, Kondo K, Imai K and Nagamiya S (2015) Acceleration of highly charged GeV Fe ions from a low-Z substrate by intense femtosecond laser. *Physics of Plasmas* **22**, 033107.
- Paul H. (2012) *The Stopping Power of Matter for Positive Ions*, *Modern Practices in Radiation Therapy* and G Natanasabapathi (ed.), ISBN: 978-953-51-0427-8, London: InTech, p. 124. Available at: <http://www.intechopen.com/books/modern-practices-in-radiation-therapy/the-stopping-power-of-matter-for-positive-ions>.
- Petrov GM, McGuffey C, Thomas AGR, Krushelnick K and Beg FN (2016) Generation of heavy ion beams using femtosecond laser pulses in the target normal sheath acceleration and radiation pressure acceleration regimes. *Physics of Plasmas* **23**, 063108.
- Petrov GM, McGuffey C, Thomas AGR, Krushelnick K and Beg FN (2017) Heavy ion acceleration in the radiation pressure acceleration and breakout afterburner regimes. *Plasma Physics and Controlled Fusion* **59**, 075003.
- Popov VS (2004) Tunnel and multiphoton ionization of atoms and ions in a strong laser field (Keldysh theory). *Physics-Uspekhi* **47**, 855.
- Qiao B, Shen XF, He H, Xie Y, Zhang H, Zhou CT, Zhu SP and He XT (2019) Revisit on ion acceleration mechanisms in solid targets driven by intense laser pulses. *Plasma Physics and Controlled Fusion* **61**, 014039.
- Robinson APL, Zepf M, Kar S, Evans RG and Bellei C (2008) Radiation pressure acceleration of thin foil with circular polarized laser pulse. *New Journal of Physics* **10**, 013021.
- Roth M, Cowan TE, Key MH, Hatchett SP, Brown C, Fountain W, Johnson J, Pennington DM, Snavely RA, Wilks SC, Yasuike K, Ruhl H, Pegoraro F, Bulanov SV, Campbell EM, Perry MD and Powell H (2001) Fast ignition by intense laser-accelerated proton beams. *Physical Review Letters* **86**, 436–439.
- Sharkov BY, Hoffmann DHH, Golubev AA and Zhao Y (2016) High energy density physics with intense ion beams. *Matter and Radiation at Extremes* **1**, 28.
- Silva IO, Marti M, Davies JR and Fonseca RA (2004) Proton shock acceleration in laser-plasma interactions. *Physical Review Letters* **92**, 015002.
- Snavely RA, Key MH, Hatchett SP, Cowan TE, Roth M, Phillips TW, Singh MA, Wilks SC, Offenberger A, Pennington DM, Yasuike K, Langton AB, Lasinski BF, Johnson J, Perry MD and Campbell EM (2000) Intense high-energy proton beams from petawatt-laser irradiation of solids. *Physical Review Letters* **85**, 2945–2948.
- Tamburini M, Pegoraro F, Di Piazza A, Keitel CN and Macchi A (2010) Radiation reaction effects on radiation pressure acceleration. *New Journal of Physics* **12**, 123005.
- Torrisi L, Gammino S, Mezzasalma AM, Badziak J, Parys P, Wołowski J, Woryna E, Krasa J, Laska L, Pfeifer M, Rohlena K and Boody FP (2003) Implantation of ions produced by the use of high power iodine laser. *Applied Surface Science* **217**, 319–331.
- Torrisi L, Gammino S, Ando L, Laska L, Krasa J, Rohlena K, Ullschmied J, Wołowski J, Badziak J and Parys P (2006) Equivalent ion temperature in Ta plasma produced by high energy laser ablation. *Journal of Applied Physics* **99**, 083301.
- Wilks SC, Langdon AB, Cowan TE, Roth M, Singh M, Hatchett S, Key MH, Pennington D, MacKinnon A and Snavely RA (2001) Energetic proton generation in ultra-intense laser-solid interactions. *Physics of Plasmas* **8**, 542.
- Wołowski J, Badziak J, Czarnecka A, Parys P, Pisarek M, Rosinski M, Turan R and Yerci S (2007) Application of pulsed laser deposition and laser-induced ion implantation for formation of semiconductor nanocrystallites. *Laser and Particle Beams* **25**, 65–69.
- Wu D, Qiao B, McGuffey C, He XT and Beg FN (2014) Generation of high-energy mono-energetic heavy ion beams by radiation pressure acceleration of ultra-intense laser pulses. *Physics of Plasmas* **21**, 123118.
- Xu Y, Wang J, Qi X, Li M, Xing Y, Yang L and Zhu W (2017) Plasma block acceleration via double targets driven by an ultraintense circularly polarized laser pulse. *Physics of Plasmas* **24**, 033108.

- Yin L, Albright BJ, Hegelich BM and Fernandez JC** (2006) GeV laser ion acceleration from ultrathin targets: the laser breakout afterburner. *Laser and Particle Beams* **24**, 291–298.
- Yin L, Albright BJ, Hegelich BM, Bowers KJ, Flippo KA, Kwan TJT and Fernandez JC** (2007) Monoenergetic and GeV ion acceleration from the laser breakout afterburner using ultrathin targets. *Physics of Plasmas* **14**, 056706.
- Yin L, Albright BJ, Jung D, Bowers KJ, Shah RC, Palaniyappan S, Fernández JC and Hegelich BM** (2011) Mono-energetic ion beam acceleration in solitary waves during relativistic transparency using high-contrast circularly polarized short-pulse laser and nanoscale targets. *Physics of Plasmas* **18**, 053103.
- Zheng FL, Wang HY, Yan XQ, Tajina T, Yu MY and He XT** (2012) Sub-TeV proton beam generation by ultra-intense irradiation of foil-and-gas target. *Physics of Plasmas* **19**, 023111.